

# Lawrence Berkeley National Laboratory

## Recent Work

**Title**

THEORY AND BACKGROUND OF FRACTURE MECHANICS

**Permalink**

<https://escholarship.org/uc/item/8992391g>

**Author**

Parker, Earl R.

**Publication Date**

1964-09-01

University of California  
Ernest O. Lawrence  
Radiation Laboratory

THEORY AND BACKGROUND OF FRACTURE MECHANICS

TWO-WEEK LOAN COPY

*This is a Library Circulating Copy  
which may be borrowed for two weeks.  
For a personal retention copy, call  
Tech. Info. Division, Ext. 5545*

Berkeley, California

## **DISCLAIMER**

This document was prepared as an account of work sponsored by the United States Government. While this document is believed to contain correct information, neither the United States Government nor any agency thereof, nor the Regents of the University of California, nor any of their employees, makes any warranty, express or implied, or assumes any legal responsibility for the accuracy, completeness, or usefulness of any information, apparatus, product, or process disclosed, or represents that its use would not infringe privately owned rights. Reference herein to any specific commercial product, process, or service by its trade name, trademark, manufacturer, or otherwise, does not necessarily constitute or imply its endorsement, recommendation, or favoring by the United States Government or any agency thereof, or the Regents of the University of California. The views and opinions of authors expressed herein do not necessarily state or reflect those of the United States Government or any agency thereof or the Regents of the University of California.

Rept. presented at American Soc.  
of Metals, Philadelphia, Oct. 19, '64.  
Also sub. for pub. in the Proceed-  
ings.

UCRL-11687 Rev. 1

UNIVERSITY OF CALIFORNIA  
Lawrence Radiation Laboratory  
Berkeley, California  
AEC Contract No. W-7405-eng-48

THEORY AND BACKGROUND OF FRACTURE MECHANICS

Earl R. Parker

September 1964

THEORY AND BACKGROUND OF FRACTURE MECHANICS

Earl R. Parker

Introduction

Fracture is a complex problem having many facets. It is highly likely that a complete understanding of fracture processes in ductile materials can only be acquired by combining the atomistic viewpoint with the mathematical theory of plasticity. Both concepts will be considered herein, and at times they will become intermixed, although it is fair to say at the outset that there is not a satisfactory solution to any fracture problem.

Nature of Fracture Processes

Of the many different kinds of fractures, only those characteristic of materials that flow plastically prior to failure will be considered herein. Fracture is a two-stage process (not a single event, as it has often been treated) consisting of (1) a crack nucleation stage and (2) a growth period wherein the crack enlarges. Even with ductile materials the fracture problem is complicated because of the fact that there are two common modes of separation, namely shear and cleavage. Furthermore, the stress state has a marked effect, particularly upon the growth stage. Under hydrostatic pressure growth is suppressed, whereas it is accentuated by an increase of the triaxial component of tensile stress. Various other factors, such as temperature and strain rate, also markedly affect fracture behavior. These factors, when combined with the complications caused by the

presence of a sharp notch, make an unambiguous, comprehensive analysis very difficult. Before attempting to describe interactions of the important parameters, each variable will be discussed separately.

Tensile Fracture of Ductile Metals. Cup-cone fractures of cylindrical tensile specimens of materials such as copper and aluminum involve the formation and growth of microcracks within the central portion of the necked-down part of the specimen.<sup>(1,2)</sup> Fractures of this kind have a rough, irregular surface, called the "cup," approximately perpendicular to the tensile axis, and a "cone," which is a smoother portion intersecting the outer surface of the specimen at an angle of about  $45^\circ$  to the tensile axis. Experimental evidence indicates rather clearly that cavities are generally nucleated by plastic flow around foreign particles. Many small cavities appear simultaneously, as is shown in Fig. 1.<sup>(1)</sup> Each cavity grows outward in all directions as straining continues, and eventually cavities join to become part of the large transverse crack forming the "cup" portion of the fracture. The fewer the foreign particles, the greater the reduction in area before separation finally occurs. For example, an oxygen-free high-purity copper will continue to deform plastically until the remaining cross-sectional area is less than ten percent of the original value. High-purity aluminum behaves in a similar manner, whereas commercial grades often break with only about 30% reduction in area. In ductile metals, little islands of material between cavities become thinner with continued straining, until local separation finally occurs. A macroscopic "crack" forms across the central portion of a tensile specimen as voids grow together, and the resulting macroscopic crack spreads radially outward until it approaches the external

surface. The last portion to fail separates on a surface making an angle of approximately  $45^\circ$  with the specimen axis. A detailed examination of ductile materials during this final stage indicates rather clearly that there is no basic change in the mechanism of the fracture, but only that the stress state becomes simpler as the crack nears completion and the fracture can terminate on a single  $45^\circ$  surface. (This region is identical in nature to the shear lip on a fractured plate specimen.) A closer examination of the rough area perpendicular to the tensile axis shows that in this region the fracture surface is not planer but that it follows a zig-zag path, with each step making an angle of  $45^\circ$  or less to the specimen axis. On each inclined plane passing through or near the axis of the specimen in the necked section, there is a steep stress gradient, with a maximum shear stress existing only near the region of minimum diameter. Cracks forming in this necked section cease to propagate after they have grown a short distance because of the steep shear stress gradient. The actual "cup" area thus consists of a series of very short inclined segments joined together to form the rough central portion of the fracture. The "cone" region is similar in nature. However, near the outer surface a  $45^\circ$  crack can become longer because of the nearly uniform shear stress. The shear stress on inclined planes in this region does not decrease as rapidly with increasing distance from the minimum section as does the stress on planes near the axis. These details are indicated schematically in Fig. 2.

More plastic deformation always occurs at the neck of the tensile specimen when hydrostatic pressure is superimposed upon the tensile load. External pressure tends to close the cavities and thus in effect it

counteracts in part the lateral growth tendency imparted to the cavities by the tensile load. This effect might be visualized by considering the case of a tensile specimen strained until numerous voids had formed in the volume comprising the necked region. If the tensile load were removed from such a specimen and a radial pressure applied, the necking would continue but the voids would be squeezed closed by the pressure. The growth characteristics of a crack thus depend upon the nature of the stress system. Tensile stresses normally tend to open cracks, whereas compressive stresses tend to close them.

Cleavage Fracture of Ductile Metals. In materials that fail after small amounts of plastic flow, the fracture process is different. In such cases, cracks nucleate because of high local stress concentrations generated by dislocations piled up because of barriers at the ends of slip bands. Examination of theoretical models shows that there are several ways in which glide dislocations can become united to form microcracks. The simplest process is that of edge dislocations being pushed together by the applied stress to form a microcrack. This is illustrated schematically in Fig. 3, and Fig. 4 is a photograph showing actual cracks of this type in a magnesium-oxide crystal. In ductile metals like copper and aluminum, dislocations do not form pile-ups because easy cross-slip permits dislocations to move out of active slip planes wherever high local stresses occur. Pile-ups or local concentrations of dislocations large enough to create microcracks can only form in materials wherein cross-slip does not occur readily. This seems to be the case with virtually all body centered cubic and hexagonal close-packed metals at low temperatures. At high temperatures, dislocations can cross-slip readily in almost all metals and,



consequently, microcracks are not nucleated by dislocations. These points will be discussed more completely in a later paragraph, after other important factors have been considered.

Dislocations on intersecting slip bands may cause microcracks to form by the process shown in Fig. 5, and the photograph in Fig. 6 shows an example of such crack formation. Also, cracks can form where a slip band intersects a grain boundary. The stress concentration effect arising from such an event is dramatically illustrated by the polarized light picture in Fig. 7, where slip lines are terminated at a grain boundary. Figures 8 and 9 are photographs showing cracks that had formed in MgO as a result of such stress concentrations. Low<sup>(3)</sup> has shown that the brittle fracture stress in unnotched specimens is exactly equal to the yield strength in compression, and that the larger the grain size, the lower the brittle fracture stress (i.e., the larger the grain size, the higher the stress concentration at the ends of a slip band). His results are reproduced in Fig. 10.

There have been very few direct observations of cracks being nucleated by dislocations in metals. Hull<sup>(4)</sup> and Honda<sup>(5)</sup> and Hornbogen<sup>(6)</sup> all observed microcracks at the intersections of twins in silicon-iron or phosphorus-iron single crystals. Honda<sup>(5)</sup> also found microcracks forming parallel to the specimen axis in crystals wherein slip occurred on two intersecting systems. Although the direct evidence that dislocation pile-ups can nucleate cracks in metals is meager, there is little room to doubt that such cracking does occur quite frequently in body centered cubic metals at low temperatures. There is convincing indirect evidence that

small amounts of impurities can have profound effects upon crack nucleation by dislocations. Zone refined iron was found by Smith and Rutherford<sup>(7)</sup> to be ductile (with 90% reduction in area) at liquid helium temperature; a few thousandths of one percent of carbon or nitrogen are known to have a marked deleterious effect upon ductility. As Mott, Stroh, and others have pointed out, metals with yield drops (due to carbon or nitrogen) are more likely to be susceptible to crack nucleation and brittle fracture. In such metals, large avalanches of dislocations are formed suddenly when yielding occurs and high local stress concentrations result.

Microcracks can also be nucleated by the fracturing of brittle inter-metallic compounds, such as  $\text{Fe}_3\text{C}$ , particularly if they are plate-like in form. Microcracks, once nucleated, may undergo limited growth; for example, across a single grain in a polycrystalline material, as shown in Fig. 11,<sup>(31)</sup> or they may grow catastrophically and cause large-scale failure. The growth behavior of a crack is influenced by both the local stress condition as well as the externally applied load. The main feature of the large-scale crack growth problem is that the energy required for this process must be supplied by the external load. In truly brittle materials only the surface energy need be provided, as was suggested by the early work of Griffith.<sup>(8)</sup> In ductile materials, the energy needed is often several orders of magnitude greater than the required surface energy because of the work associated with the local plastic flow at the tip of the advancing crack. This problem has been considered by Irwin,<sup>(9)</sup> Orowan,<sup>(10)</sup> Gilman,<sup>(11)</sup> and others; it will be treated in detail in a later section. Gilman<sup>(11)</sup> measured the effective surface energy for crack propagation in

single crystals of zinc and in silicon iron at various temperatures.

Using a mechanical arrangement in which the force required to propagate an existing cleavage crack could be measured, he obtained the results for zinc shown in Fig. 12. The surface energy for zinc was found to drop rapidly with decreasing temperatures; this was also the case for silicon iron.

Grain Size. One of the most important metallurgical variables influencing brittle behavior is grain size. With larger grain sizes, the slip distance increases, the stress concentration at the end of the slip band becomes larger, and the probability of crack nucleation becomes greater. This effect was illustrated in Fig. 10. In addition to the effect of grain size on crack nucleation, there is also an effect on growth. As cleavage cracks cross grain boundaries, showers of dislocations are created, branching of cracks occurs, and cleavage steps are formed. All of these events cause the energy per unit of fracture surface to increase. Thus, small grained material, in which boundary crossing is more frequent than in larger grained specimens, should logically be expected to absorb more energy.

#### The Effects of Strain Rate and Temperature

Strain Rate. Stress-strain curves for most metals are raised when the strain rate is increased, but large changes in strain rate are required to produce a significant evaluation in the stress-strain curve. The sensitivity to strain rate varies widely for different materials, being largest for body centered cubic metals such as iron and smallest for face centered cubic metals such as copper. Although strain-rate data are not

extensive, enough information is available to indicate clearly the nature and magnitude of the strain-rate effect. Figure 13 shows how changes in strain rate influence the room temperature tensile properties of mild steel.<sup>(12)</sup> At low strain rates there is little effect upon yield strength, but at high strain rates the yield strength is increased by 10% or more for each factor of ten increase in strain rate. Other investigators<sup>(13, 32, 33)</sup> have reported somewhat different results, indicating that there is a more uniform increase in strength with increasing strain rate over the entire range. However, in all cases, the 10% increase in yield strength for each ten-fold increase in deformation rate is a good approximation of the strain-rate effect for medium strength steels. In sharp contrast is the behavior of copper, which does not exhibit any increase in yield strength when the strain rate is varied by 100,000 times.<sup>(14)</sup> The behavior of aluminum alloys is intermediate between those of steel and copper. The strain-rate effect becomes less as the test temperature is lowered below room temperature.

The rate sensitivity arises from the fact that in most metals the mobility of dislocations is temperature dependent. Local stresses produced by thermal vibrations of the lattice play an important part in the plastic behavior of most metals.<sup>(15, 16)</sup> The probability that the thermal stress will be able to assist the load stresses in moving dislocations is greater with longer times or higher temperatures. At any given temperature thermal energy contributes more to plastic flow when the strain rate is low because there is little time for thermal energy to affect dislocations at high strain rates. It is for this reason that plastic

stress-strain curves of ductile metals are raised by increasing the strain rate. This effect has a very important influence on the brittle behavior of ductile metals, particularly the body centered cubic ones. Additional comments will be made about this subject in the subsequent discussion related to the behavior of notched bars and plates.

Effect of Temperature. The yield strength of metals increases as the temperature decreases, but the amount of the change varies for different materials. Figure 14 shows how the tensile properties of structural steel change with decreasing temperature. Comparisons of different metals have been made in Fig. 15, where the ratio of the yield strength at various temperatures is shown as a function of yield strength at absolute zero (corrected for differences in modulus of elasticity due to temperature). The temperature dependence of yield strength is related to the strain-rate effect.<sup>(14)</sup> The equivalence between changes in strain rate and temperature changes, which involve rather complex dislocation concepts and analyses, will not be discussed in detail here because it would not contribute significantly to the main theme of the paper. The general influences of changes in strain rate and temperature, as discussed above, are adequate background for the subsequent discussions.

#### The Behavior of Notched Bars and Plates

The Griffith Approach. Early in the 1920's Griffith developed the concept that a pre-existing crack can only extend when the amount of elastic strain energy released upon growth of the crack equals or exceeds the surface energy of the newly formed crack.<sup>(8)</sup> Although this concept was restricted by Griffith to the fracture of truly brittle materials such as

glass, it has been extended to include the case of brittle fracture of metals<sup>(28,29)</sup> by substituting a plastic work term for the surface energy term in the Griffith formula relating crack propagation stress, modulus of elasticity, surface energy, and crack length. Because this concept is basic in present-day testing and evaluating of materials, its development will be traced herein.

Griffith used the analysis developed by Inglis<sup>(17)</sup> for the stress distribution around an elliptic crack in a thin plate of infinite length and width. Griffith considered the case where the ellipse was degenerated into a thin crack that could extend when the total energy in the system remained unchanged as the crack grew.

The Inglis analysis provided a solution for the stress distribution around an internal crack, with the maximum stress being given by

$$\sigma_{\max} = 2\sigma_0 \sqrt{c/\rho}$$

where  $\sigma_0$  is the applied stress remote from the crack,  $2c$  is the crack length, and  $\rho$  is the radius of curvature at the ends of the major axis of the elliptical crack. Because  $\sigma_{\max}$  cannot be determined without knowing the generally unmeasurable quantity,  $\rho$ , Griffith developed an analysis based upon energy considerations. From the stress distribution around an elliptical crack, Griffith calculated the elastic energy per unit of volume stored in the material just ahead of the crack. He obtained the following for a plate of unit thickness

$$U_e = \pi c^2 \sigma_0^2 / E$$

where  $U_e$  is the elastic energy stored in the plate ahead of the crack front,  $E$  is Young's modulus, and the other terms are the same as before.

(The solution for a surface crack of depth  $c$  is approximately the same.)

The above expression is applicable only to thin plates where the thickness direction stress is zero, a condition called plane stress. For thick plates, wherein thickness direction stresses develop as a consequence of non-uniform Poisson's ratio contraction at the apex of the notch, the thickness direction strain is considered to be equal to zero (this state is called plane strain), the strain energy per unit of thickness is given by

$$U_e = (1 - \nu^2) \pi c^2 \sigma_o^2 / E$$

where  $\nu$  is Poisson's ratio.

The surface energy (per unit of thickness) of a crack  $2c$  in length is given by  $U_s = -4\alpha c$  where  $\alpha$  is the surface energy per unit of area. A crack will become unstable when the stored elastic energy is equal to or greater than the energy needed to create the new crack surface formed when the crack extends. Thus

$$\frac{d}{dc}(U_e + U_s) = \frac{d}{dc} \frac{\pi c^2 \sigma_o^2}{E} - 4\alpha c = 0$$

or

$$\frac{2\pi c \sigma_o^2}{E} = 4\alpha$$

which leads to the familiar Griffith relation

$$\sigma_o^2 = \frac{2\alpha E}{\pi c}$$

The appropriate expression for thick plates (the plane strain case) is

$$\sigma_o^2 = \frac{\alpha E}{\pi c(1-\nu)^2}$$

The terms  $\frac{\pi c \sigma_o^2}{E}$  and  $2\alpha$  are energy release rate terms, denoted by  $G$  in current terminology. Thus

$$G = 2\alpha = \frac{\pi c \sigma_o^2}{E} \quad \text{for plane stress}$$

and

$$G_I = \frac{\pi c \sigma_o^2 (1-\nu^2)}{E} \quad \text{for plane strain}$$

where the subscript I has been added to  $G$  to distinguish the plane strain case from that of plane stress.

These expressions cannot be applied without modification to specimens of finite dimensions. Irwin<sup>(18)</sup> used a method of analysis developed by Westergaard<sup>(19)</sup> for determining the modification needed for a specimen of finite width,  $W$ . He obtained the following relationship for the energy release rate

$$G = \frac{\sigma_o^2 W}{E} \tan \frac{\pi c}{W}$$

The Westergaard analysis leads to the following equations for stress in the vicinity of a crack apex:



$$\sigma_y = \frac{\sigma_o}{\sqrt{2r/c}} \cos \frac{\theta}{2} \left[ 1 + \sin \frac{\theta}{2} \sin \frac{3\theta}{2} \right]$$

$$\sigma_x = \frac{\sigma_o}{\sqrt{2r/c}} \cos \frac{\theta}{2} \left[ 1 - \sin \frac{\theta}{2} \sin \frac{3\theta}{2} \right] \quad \text{---} \sigma_{ox}$$

$$\tau_{xy} = \frac{\sigma_o}{\sqrt{2r/c}} \sin \frac{\theta}{2} \cos \frac{\theta}{2} \cos \frac{3\theta}{2}$$

where  $\sigma_z = 0$  for plane stress or  $\sigma_z = \nu(\sigma_x + \sigma_y) = \frac{2\nu\sigma_o}{\sqrt{2r/c}} \cos \frac{\theta}{2}$  for plane strain where  $\sigma_y$  is the stress due to the load acting perpendicular to the notch,  $\sigma_x$  is the stress due to a load parallel to the notch,  $\sigma_z$  is the induced thickness direction stress,  $r$  and  $\theta$  are polar coordinates (based upon the apex of the notch as the origin),  $r$  being the distance to any point in the plate, and  $\theta$  being the angle between  $r$  and the line of the notch. The general nature of such a stress distribution is illustrated by the photoelastic pattern shown in Fig. 16. Making certain simplifying assumptions, Irwin was able to use the Westergaard analysis to calculate the relative sizes of the plastic zones for plane stress and plane strain states. These results are reproduced in Fig. 17. Although calculations of this type are not sufficiently accurate to permit a close quantitative prediction of the behavior of a material, the results do show that the energy release rate for plane strain conditions is substantially lower than that for the plane stress state because of the larger plastic zone associated with the latter.

In addition to the energy release rates,  $G$  and  $G_I$ , stress criteria for failure,  $K$  and  $K_I$ , are often employed as measures of the notch

toughness of materials. The relationship between the two sets of parameters will be demonstrated next.

Equivalence of the Energy and Stress Criteria. The cohesion between atom planes can be estimated in the following manner. When a crystal breaks by cleavage, two new surfaces are formed and the energy per unit of area required to create them is  $2\alpha$ , where  $\alpha$  is the surface energy. The force involved in separating the atom planes is opposed by interatomic attractive forces. Figure 18 shows how the atomic force per unit of area varies with the separation distance,  $d$ , between the planes being pulled apart. The force is zero at the equilibrium atomic spacing,  $b$ ; it rises to a maximum,  $\sigma_m$ , which is the cohesive stress of the material, and then falls to zero as the separation distance becomes large. The area under the curve is the fracture energy and must equal or exceed  $2\alpha$ . For an order of magnitude estimate, Hooke's law can be assumed to hold up to a stress value of  $\sigma_m$ . The elastic energy stored in the volume between a unit area of the two planes of atoms being separated is thus

$$b \sigma_m^2 / 2E$$

where  $b$  is the interatomic spacing. Assuming that the shaded area is half of the total area under the curve, then

$$b \sigma_m^2 / 2E = \alpha$$

The cohesive strength is thus given by

$$\sigma_m = \sqrt{2E\alpha/b}$$

A value for the cohesive stress,  $\sigma_m$ , can also be obtained from the Inglis analysis, as was previously pointed out. It is

$$\sigma_m = 2\sigma_o \sqrt{c/\rho}$$

where  $c$  is the half length of an internal crack,  $\rho$  is the radius of the crack tip, and  $\sigma_o$  is the applied stress. As indicated by Fig. 18, Hooke's law is not obeyed for large strains, and when the increase in atomic spacing approaches the value of  $b$ , the stress-strain curve flattens out. The assumption can thus be made for an order of magnitude approximation that the radius of curvature approaches  $b$  as a minimum value. Thus the maximum stress becomes

$$\sigma_{max} = 2\sigma_o \sqrt{c/b}$$

Equating the two values for  $\sigma_{max}$

$$2\sigma_o \sqrt{c/b} \approx \sqrt{2E\alpha/b}$$

or

$$\sigma_o \approx \sqrt{E\alpha/2c}$$

which differs from the Griffith equation only by a small numerical factor. With a more accurate analysis the proportionality constants would be in better agreement, but this is unimportant - the variable terms are identical, and to demonstrate this identity is the point of analysis.

The fact that the Griffith equation can be derived from elastic theory shows that a criterion for fracture based on stress is as valid as the one based on energy. A stress criterion,  $K$ , can thus be established which is proportional to the applied stress,  $\sigma_o$ . Thus

$$K \propto \sigma_0$$

or

$$K^2 \propto \sigma_0^2$$

or

$$K^2 = \pi c \sigma_0^2$$

(A more detailed analysis would show that the proportionality constant is  $\pi c$ .) Thus  $K^2 = GE$ .

Plastic Work Term. The foregoing analyses involve the application of classical theory of elasticity and therefore apply only to isotropic materials that behave in a linear elastic manner. In the brittle fracture of ductile metals, some plastic flow always occurs near the fracture surface. Irwin<sup>(9)</sup> and Orowan<sup>(10)</sup> have suggested that a plastic work term should be added to the surface tension in the Griffith equation. The energy absorbed in plastic flow has been called by various names such as "plastic surface work" and "crack propagation energy," but the term generally used is "fracture toughness." The symbols used to designate fracture toughness,  $G_c$  or  $G_{Ic}$ , are due to Irwin. Experiments have repeatedly demonstrated that the value of  $G_c$  is many orders of magnitude larger than the surface tension,  $\alpha$ , and so the Griffith equation has been reduced to the following for fractures involving plastic flow:

$$\sigma_c = \sqrt{E G_c / \pi c}$$

The critical stress,  $\sigma_c$ , necessary to cause an internal crack of length  $2c$  to propagate spontaneously is the average stress in the material remote from the crack.

In principle, the fracture toughness parameter,  $G_c$ , should be a unique value for a given material. It could be evaluated by progressively loading any specimen (having a suitable geometric form) until rapid fracture ensues. From the critical load applied at the onset of rapid crack propagation and the corresponding crack length,  $G_c$  could be calculated. Unfortunately, however, experimental work has shown that  $G_c$  is not a constant for a given material but varies with specimen geometry. Attempts to apply corrective terms<sup>(20)</sup> have not been entirely successful. Some of the reasons for this difficulty will be discussed in the following section, although the comments made therein should not be interpreted in a negative manner. Fracture mechanics, as described above, has provided the basis for understanding and solving such major fracture problems as the bursting of the de Havilland Comets, the fracture of large electric generator rotors, and the fracture of large solid propellant rocket motor chambers.

Interaction of Important Factors

Characteristic Features of Plate Fractures. One of the reasons that unique values of  $G_c$  or  $K_c$  are not found experimentally is that the nature of the fracture changes as the crack progresses from the apex of a notch across a plate. Blum<sup>21</sup> has described this complication in a clear and concise manner. Figure 19, taken from his work, illustrates the various features found on fracture surfaces. At the tip of the notch a flat fracture (usually of the shear type) forms. It originates at midthickness and grows outward as well as inward. The effect of this initial crack is twofold - it increases the crack length,  $c$ , and provides a smaller radius,  $\rho$ , at the new end of the opening. Both factors increase the stress concentration and tend to accentuate brittle behavior. In steels tested at intermediate temperatures, these alterations in crack geometry cause the fracture to change from shear to cleavage, and thus the energy needed to keep the crack moving ( $G_c$ ) suddenly drops to a low value. The growth rate of the crack increases and, at times, approaches the theoretical maximum of about 6000 feet per second. When the plate is thick (e.g., a half inch or more in thickness) and the temperature is low, such behavior is normal. At high temperatures, however, the crack tends to spread slowly across the plate. The specimen tears apart by the shear mechanism of failure, and the energy absorption is high. At intermediate temperatures the fracture will be a mixture of shear and cleavage, with an initial shear region at the origin, a cleavage portion at the midthickness, and shear lips near the two surfaces, as shown in Fig. 19. In the lower part of this figure, the amount of shear lip is indicated as a function of crack extension and plate thickness; actual test data are

shown in Fig. 20. (22)

The energy absorbed per unit of area at any crack position is primarily determined by the amount of shear fracture present. The state of stress when a shear lip forms is essentially that of plane stress, and so the  $G_c$  term is the appropriate one to consider for this portion of the fracture area. The initial part of the fracture, at the tip of the machined crack, is generally shear in nature but it differs from the lip portion in that it forms under conditions of plane strain. The term  $G_{Ic}$  can be used to differentiate this lower energy type of shear failure. In appearance, this region looks like the area of the "cup" in a broken unnotched tensile specimen, and the mechanism of failure is essentially the same. There are no new kinds of fractures to be found in notched plate; every type observed in plates can be produced in unnotched tensile specimens. The fractures in plates differ in that mixtures of the various types are frequently found in a single plate, and the amounts of each kind depend upon the thickness of the plate, the sharpness of the notch, the length of the crack, the temperature of testing, and the loading rate employed.

Even with a given kind of fracture, such as shear in a ductile tensile specimen, the amount of energy absorbed prior to fracture can vary over a wide range depending upon the stress state, as the hydrostatic tests of Bridgeman adequately demonstrated. To expect to obtain a value for fracture toughness ( $G_c$  or  $G_{Ic}$ ) that is unique for a material (regardless of specimen geometry or testing conditions) is an expectation that cannot be realized. It is within the realm of possibility, though, to make a valid analysis of the behavior of a material which would include

geometry, strain rate, and temperature effects as well as the use of tensile test data. Such an analysis could lead to a quantitative correlation of the important factors affecting notch toughness of materials. A good start has been made on this complex and difficult problem by Gerberich,<sup>(23)</sup> Swedlow and Gerberich,<sup>(24)</sup> and by Krafft,<sup>(32,33)</sup> but much work yet remains to be done. For the present, at least, the approach to notch toughness problems must remain qualitative, although there is no fundamental reason why, with sufficient effort, a valid quantitative analysis could not be developed.

Thick notched plates of ductile materials, such as copper and aluminum, also develop complex appearing fractures when broken. However, this case is simpler than that of steel because cleavage failures do not occur in such materials. Fractures in such materials consist of a flat portion, like the area of the "cup" in an ordinary tensile specimen, and a shear lip. Because of the thickness direction stress that develops in thick plates, the amount of plastic flow that occurs at the midthickness of the plate prior to fracture can be relatively small, and the notch toughness ( $G_{Ic}$ ) can be very low even for the face centered cubic metals.

Effect of Specimen Geometry. The effect of plate thickness has just been described. The plate width factor is more amenable to rational analysis than is the thickness effect. Data from a variety of sources were collected and analyzed by Jackson and coworkers,<sup>(25)</sup> and a summary plot taken from their work is reproduced in Fig. 21. They found that the stress at the onset of rapid crack propagation,  $\sigma_{G_c}$ , decreased rapidly as the



crack length was increased in plates of constant width. For example, in one-sixteenth inch thick by 35 inch wide plates of 7075-T6 aluminum alloy, the nominal fracture stress dropped from 45 percent to about 15 percent of the tensile yield stress when the crack length was changed from 3 inches to 12 inches. Furthermore, all strength values fell on a single line for a given material regardless of the width of the test specimen. Thus it was possible to represent the width effect by a single line in Fig. 21, where  $c/c_0$  was used as the abscissa (with  $c_0$  being taken as one inch).

Even in thin plates, part through cracks tend to develop plane-strain conditions because of the severe restraint imposed upon the crack. As illustrated in Fig. 22, a part through crack will often exhibit two stages of growth. In the first the crack suddenly propagates through the thickness, forming a "through" crack. This occurs at a relatively low stress level, corresponding to  $K_{Ic}$  (or  $G_{Ic}$ ). The final growth in the width direction is that normal for thin plates, namely the plane-stress type.

Part-through cracks in thicker plates may also propagate in two stages, although the tendency toward a single kind of growth increases as the thickness becomes greater. At intermediate thicknesses the fracture may be of mixed types, as indicated in the lower part of Fig. 22.

Strain-Rate Effect. Although the literature on strain rate effects in unnotched specimens is extensive, there are very little data for notched bars. It might be anticipated that because an increase in strain rate increases the yield strength of most materials (i.e., time is required for extensive plastic flow at a given stress level) that loading rate would

have a significant effect upon notch toughness. The meager information available indicates that notch bar strength (and toughness) can be markedly lowered by a large increase in strain rate.<sup>(32)</sup> Some materials show this effect while others do not (for the few cases available for study). Without more precise information, quantitative evaluations are impossible. The strain rate factor is, however, important and will require more detailed investigation.

#### Summary

Ductile materials can exhibit several modes of transcrystalline fracture, even under uniaxial tensile loading. Although there are only two basic kinds of separation processes, shear and cleavage, the presence of notches can modify either mode so that the energy absorbed (i.e., notch toughness) prior to fracture is markedly altered. Notch toughness, as measured by  $G_c$  or  $K_c$ , depends upon the volume of material that has been plastically deformed prior to fracture. The specimen geometry, the temperature of testing, and the strain rate all affect the energy absorption. Thicker plates, sharper notches, lower temperatures, and higher loading rates all tend to decrease the volume of plastically strained material and thus lower notch toughness.

Fractures in plates are often of mixed types, with the amount of each varying as the crack grows. This fact, as well as others, makes it impossible to establish a unique value of  $G_c$  for a given material. Quantitative mathematical approaches to this problem have been attempted, but they have met with limited success. However, the problems, while complex, should be soluble. Quantitative analyses should eventually be developed which would permit the prediction of notch toughness from

fundamental considerations such as tensile data, specimen geometry, temperature, and strain rate.

References

1. Puttick, K. E., Phil Mag., Vol. 4, p. 964 (1959).
2. Rogers, H. C., Trans. AIME, Vol. 218, p. 498 (1960).
3. Low, J. R., I.U.T.A.M., Madrid Colloquium, Deformation and Flow of Solids, Springer, Berlin, p. 60 (1956); Relation of Properties to Microstructure, ASM, Metals Park, Ohio, p. 163 (1954).
4. Hull, D., Acta Met., Vol. 8, p. 11 (1960).
5. Honda, R., Jour. Phy. Soc., Japan, Vol. 16, p. 1309 (1961).
6. Hornbogen, E., Trans. AIME, Vol. 221, p. 711 (1961).
7. Smith, R. L. and Rutherford, J. L., Franklin Inst. Report I A1878-1 (Feb. 1956); Acta Met., Vol. 5, p. 761 (1957).
8. Griffith, A. A., Phil. Trans. Roy. Soc., London, A, Vol. 221, p. 163 (1921); Proc. Int. Conference for Appl. Mech., p. 55 (1924).
9. Irwin, G. R., Fracturing of Metals, ASM, Metals Park, Ohio (1948).
10. Crowan, E., Reports on Progress in Physics, Vol. 12, p. 185 (1949); Fatigue and Fracture of Metals, John Wiley and Sons, N.Y. (1950).
11. Gilman, J. J., Jour. Appl. Phys., Vol. 31, p. 2208 (1960):
12. Manjoine, M. J., Jour. Appl. Mech., Vol. 11, No. 4 (1944).
13. Hollomon, J. H. and Jaffe, L. D., Ferrous Metallurgical Design, John Wiley and Sons, N.Y. (1947).
14. Baron, H. G., Jour. I.S.I., Vol. 182, p. 354 (1956).
15. Cottrell, A. H., Dislocations and Plastic Flow in Crystals, Oxford at Clarendon Press, London (1953).
16. Seeger, A., Diehl, J., Mader, S. and Rebstock, H., Phil Mag., Vol. 2, p. 323 (1957).

17. Inglis, C. E., Trans. Inst. Naval Architects, London, Vol. LV, p. 219 (1913).
18. Irwin, G. E., Materials For Missiles and Spacecraft, McGraw-Hill, N.Y. (1963).
19. Westergaard, H. M., Trans. Amer. Soc. Mech. Engr., Vol. 61, p. A49 (1939).
20. Irwin, G. R., Proc. First Symposium on Naval Structural Mechanics, Stanford University, Stanford, Calif., p. 557 (1958).
21. Blum, J. I., Proc. ASTM, Vol. 61, p. 1324 (1961); Vol. 62 (1962).
22. Irwin, G. R. and Kies, J. A., Proc. Golden Gate Metals Conference, San Francisco, p. 79 (1960).
23. Gerberich, W. W., Plastic Strains and Energy Density in Cracked Plates, Part I. Presented at Soc. Exp. Stress Analysis Meeting, Salt Lake City, Utah, May 6-8, 1964.
24. Swedlow, J. L. and Gerberich, W. W., Plastic Strains and Energy Density in Cracked Plates, Part II, Presented at Soc. Exp. Stress Analysis Meeting, Salt Lake City, Utah, May 6-8, 1964.
25. Jackson, L. R., McClure, G. M., and Kasuba, J. A., DMIC Memo. 174, Battelle Mem. Inst., Columbus, Ohio, August, 1963.
26. Stokes, R. J., Johnston, T. L., and Li, C. H., Phil Mag., Vol. 4, p. 920 (1959).
27. Johnston, W. G., Phil Mag., Vol. 5, p. 407 (1960).
28. Ku, R. and Johnston, T. L., Phil Mag., Vol. 9, p. 231 (1964).
29. Johnston, T. L., Stokes, R. J., and Li, C. H., Phil Mag. Vol. 7, p. 23 (1962).

30. Johnston, T. L. and Parker, E. R., Fracture of Solids, Interscience Publishers, N.Y. (1963), p. 267.
31. Low, J. R., Fracture, John Wiley and Sons, N.Y., (1959), p. 68.
32. Krafft, J. M. and Sullivan, A. M., ASM Trans., 56, 160 (1963).
33. Krafft, J. M., Appl. Materials Res., 2, (1963).

Figure Captions

1. Section through the neck of a tensile specimen of as-rolled tough pitch copper, tested at room temperature; grain size 0.05 mm. 9X (K. E. Puttick<sup>(11)</sup>).
2. Sketch illustrating some of the important details involved in the fracturing of a tensile specimen of ductile metal.
3. Sketch illustrating how edge dislocations can be forced together to form a microcrack perpendicular to a slip band.
4. Photomicrograph showing microcracks at the intersections of slip bands in the tension side of a bent MgO single crystal. 150X (R. J. Stokes, T. L. Johnston, and C. H. Li<sup>(26)</sup>).
5. Sketch illustrating how a microcrack can form within a slip band.
6. Photomicrograph showing a microcrack within a slip band, nucleated by the stress concentration created at the intersection of two slip bands. 350X (W. G. Johnston<sup>(27)</sup>).
7. Polarized transmitted light photomicrograph of a MgO bicrystal showing stress concentrations at the ends of slip bands. 80X (R. Ku and T. L. Johnston<sup>(28)</sup>).

8. Photomicrograph showing a microcrack caused by the stress concentration at the intersection of a slip band and a grain boundary. 500X  
(T. L. Johnston, R. J. Stokes, and C. H. Li<sup>(29)</sup>)
9. Photomicrograph showing multiple microcracks formed at intersections of slip bands and a grain boundary. <sup>(30)</sup> 500X
10. Effect of grain size on yield stress in compression and cleavage stress in tension, medium carbon structural steel tested at  $-196^{\circ}\text{C}$ .  
(J. R. Low<sup>(3)</sup>)
11. Photomicrograph showing a plastically deformed grain between two others having cleavage microcracks. Polycrystalline iron strained 7.5% in bending at  $78^{\circ}\text{K}$ . (J. R. Low<sup>(31)</sup>)
12. Measured values of surface energy as a function of temperature for zinc and a zinc alloy. (J. J. Gilman<sup>(11)</sup>)
13. Effect of strain rate upon the tensile properties of medium carbon structural steel at room temperature. (M. J. Manjoine<sup>(12)</sup>)
14. The effect of testing temperature on the tensile yield strength and true fracture stress of a hot-rolled semikilled 0.2% carbon steel.
15. Effect of temperature on the tensile yield strength of several materials; yield strength at temperature  $T$  divided by yield strength at absolute zero plotted as ordinate.



16. Polarized light photograph showing stress pattern in an internally notched plate. (Courtesy of A. McEvily)
17. Relative size of plastic zones for plane-stress and plane-strain states in a notched plate. (G. R. Irwin and J. A. Kies<sup>(22)</sup>)
18. Sketch illustrating the nature of the stress vs separation distance for atom planes in a crystal.
19. Sketch illustrating the complex nature of fracture in notched plates, and the effect of plate thickness on the % shear on the fracture surface. (J. I. Blum<sup>(21)</sup>)
20. The effect of plate thickness on fracture toughness of steel. (G. R. Irwin and J. A. Kies<sup>(22)</sup>)
21. Effect of plate width and crack size on nominal strength of thin plates of various aluminum alloys and on 17-7PH steel. (L. R. Jackson, G. M. McClure, and J. A. Kasuba<sup>(25)</sup>)
22. Sketch illustrating effect of part-through notch on thin and thick plates. Crack starts as a plane-strain failure in thin plates and then propagates as a plane-stress crack.



ZN-4534

Fig. 1.

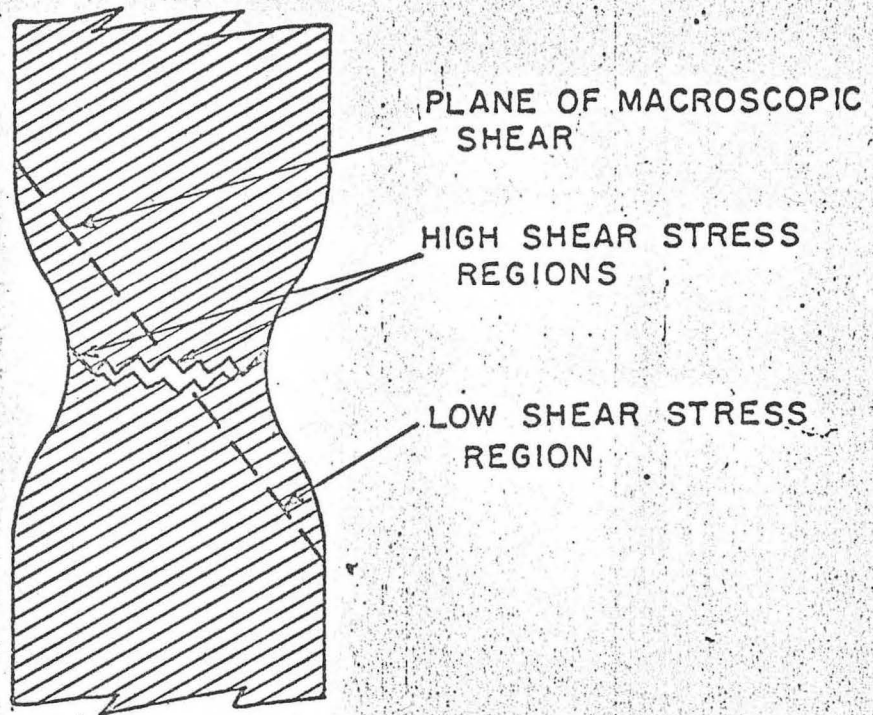


Fig. 2.



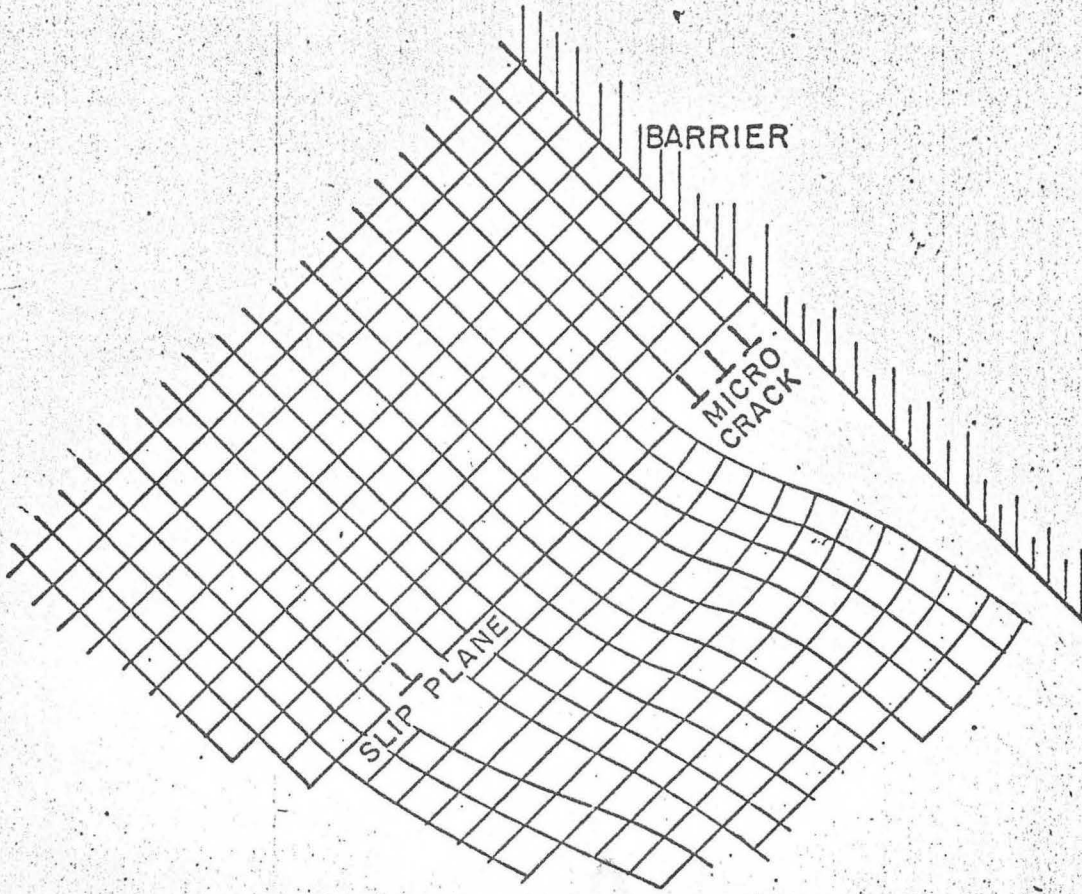
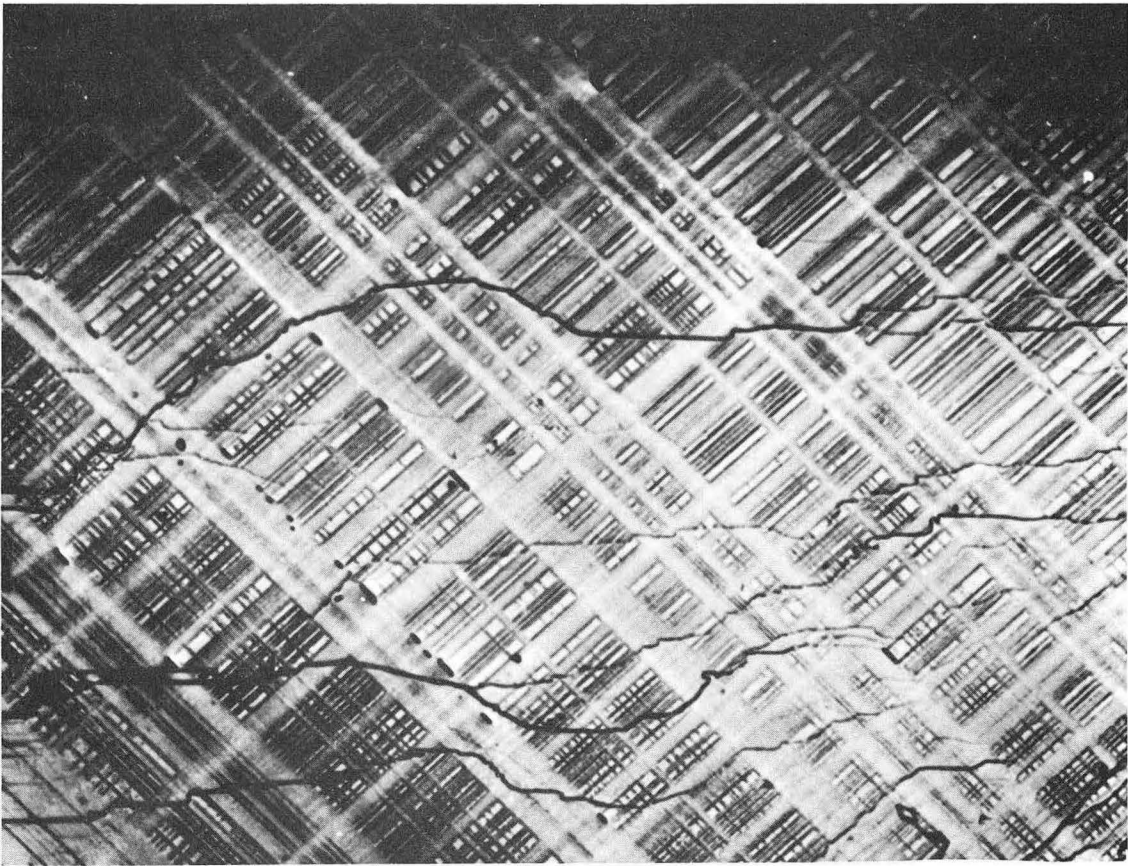


Fig. 3.



ZN-4535

Fig. 4



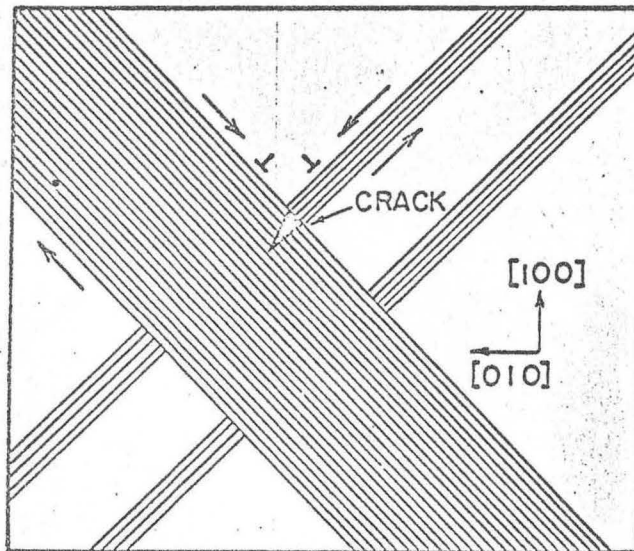
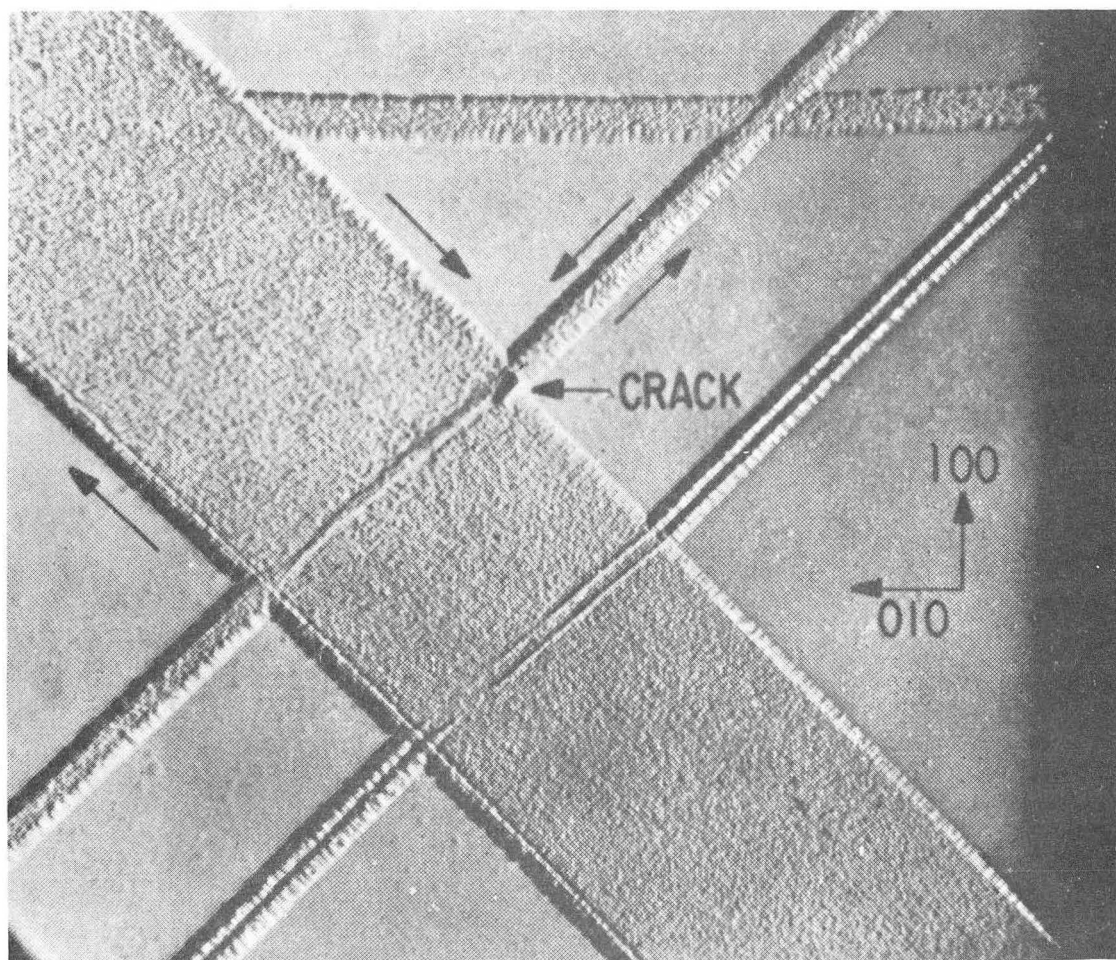
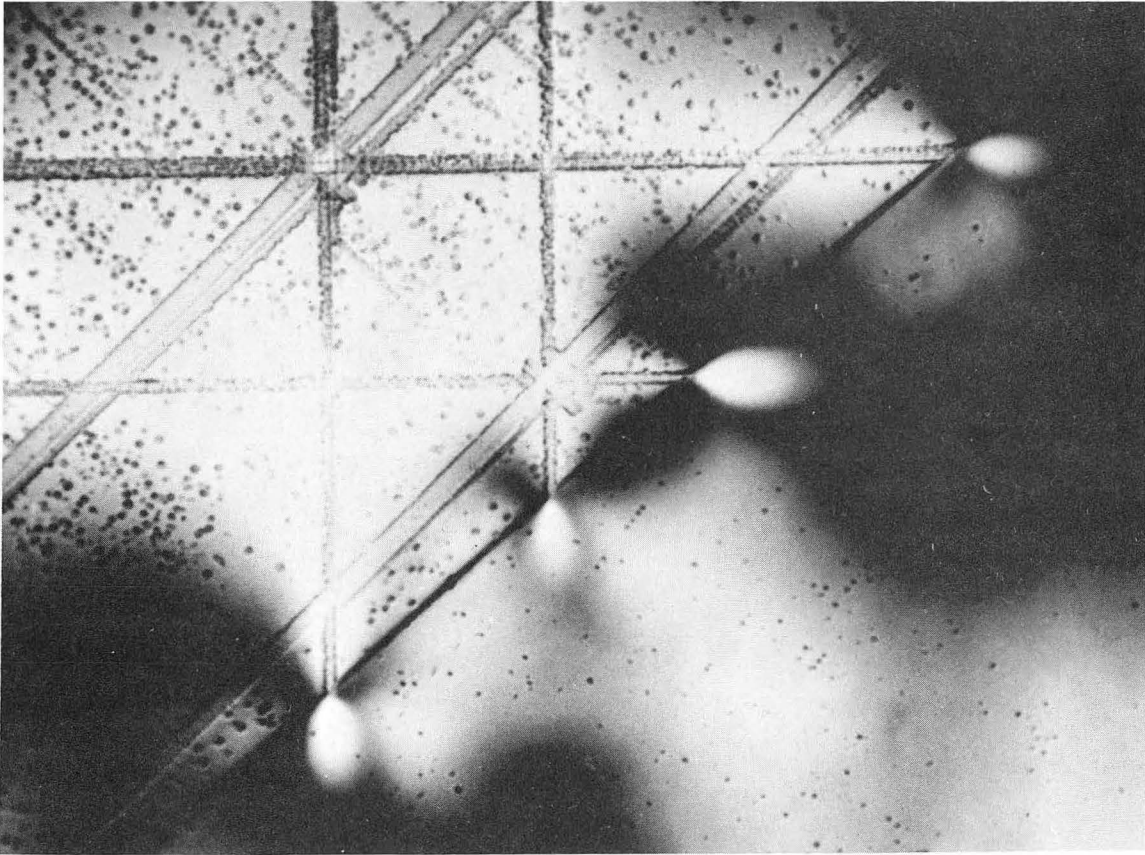


Fig. 5.



ZN-4533

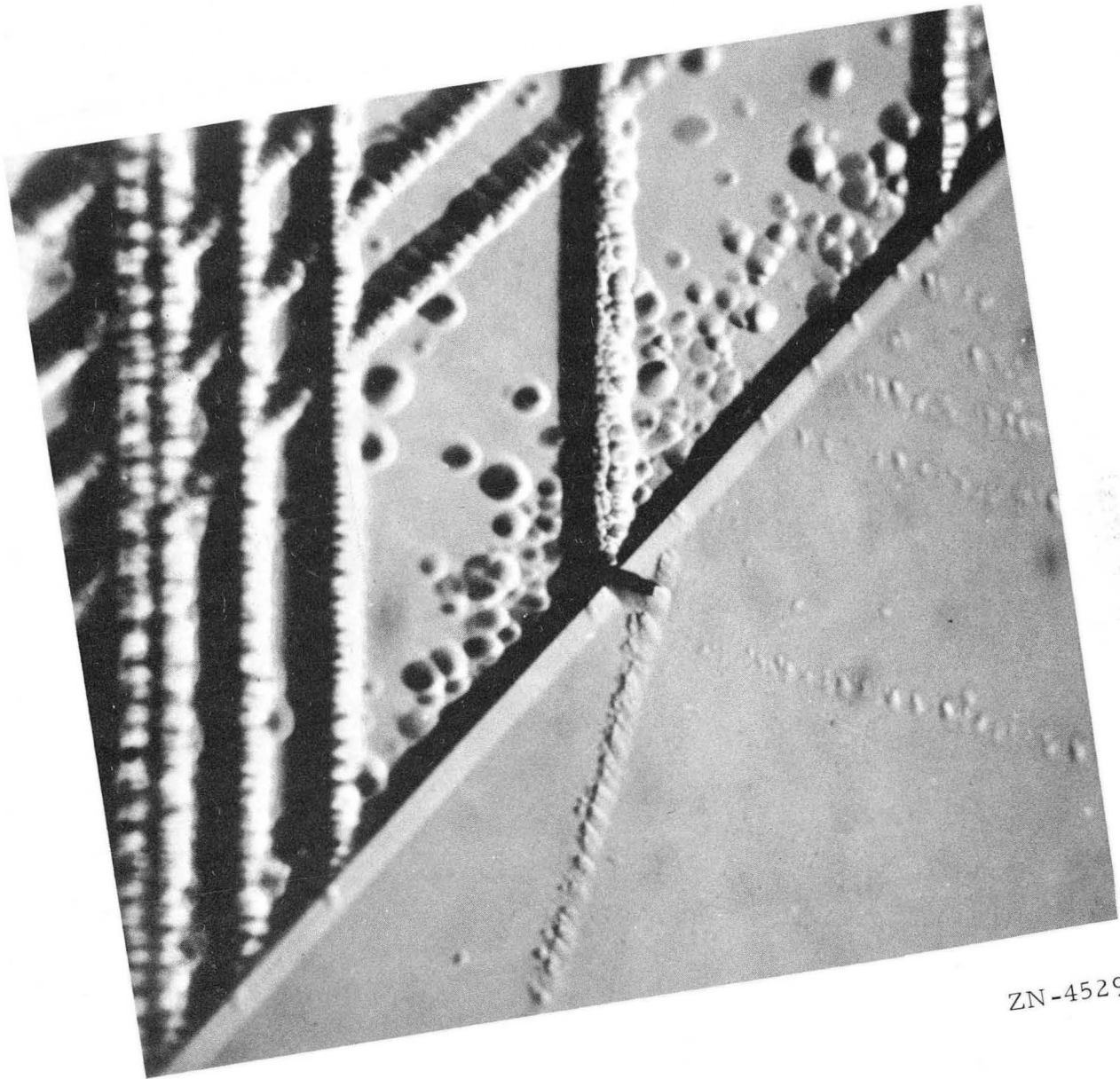
Fig. 6



ZN-4531

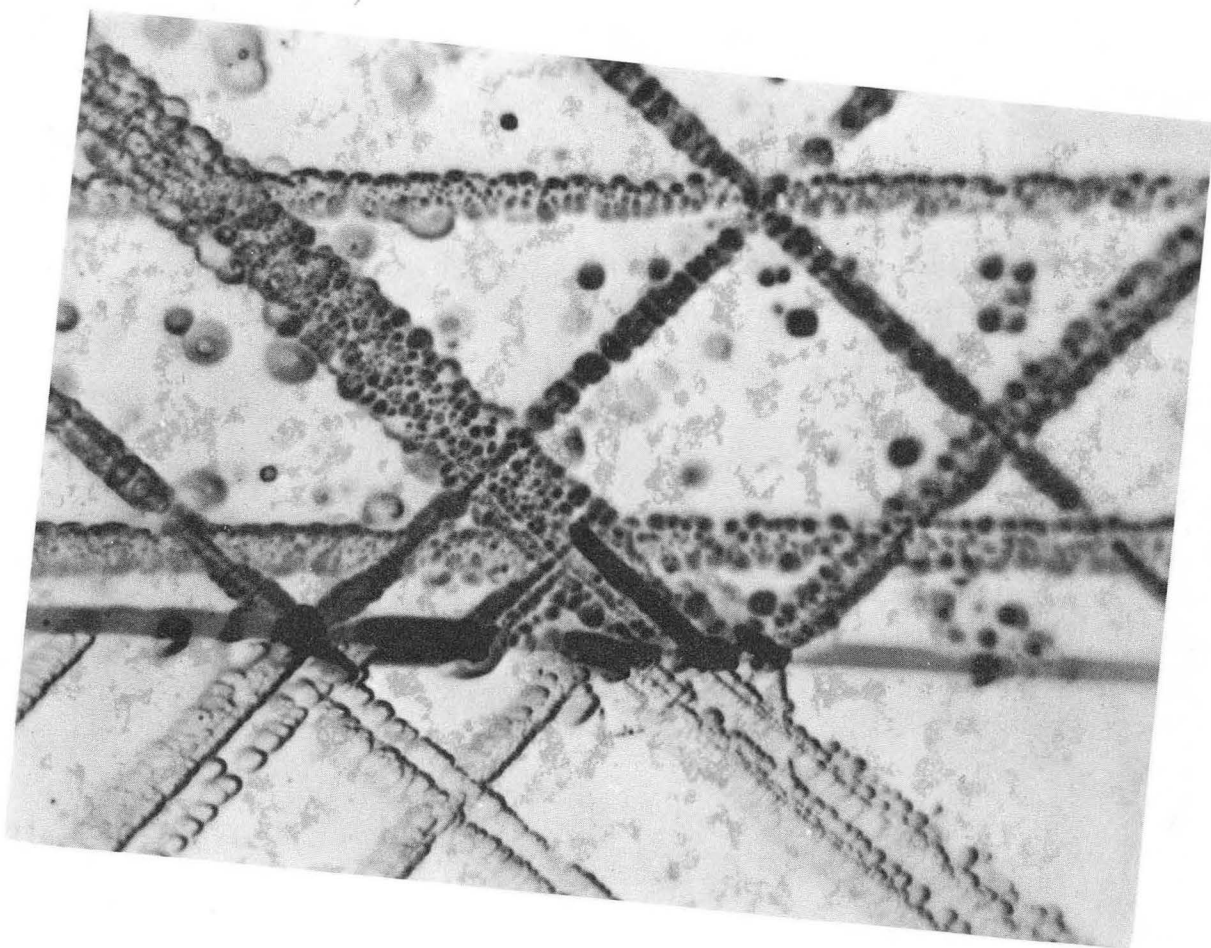
Fig. 7





ZN-4529

Fig. 8



ZN-4530

Fig. 9

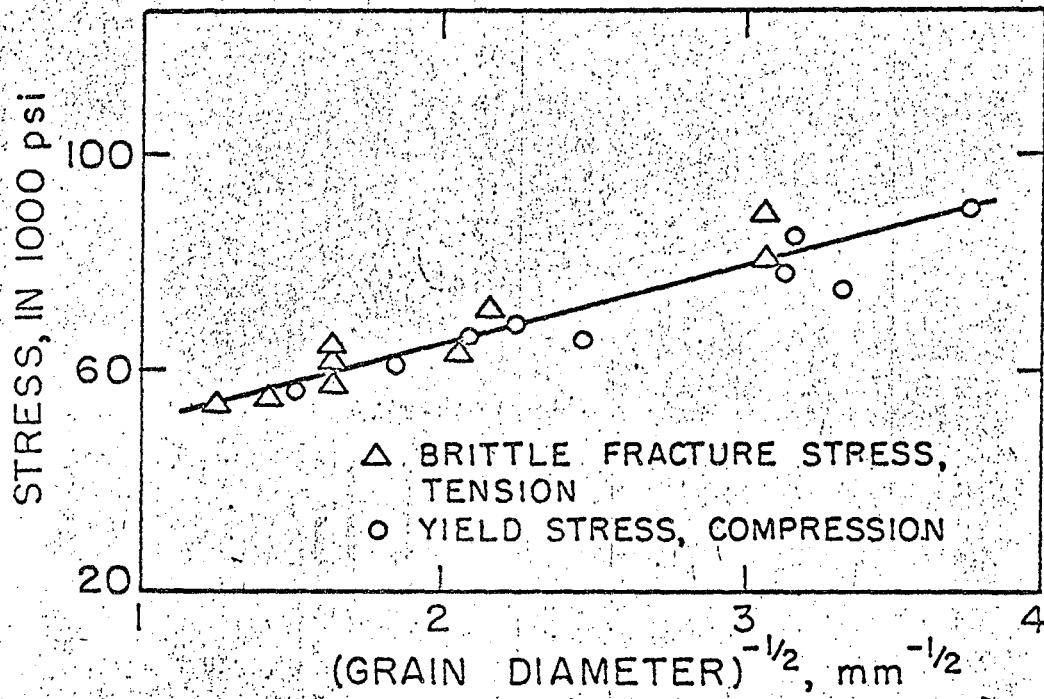


Fig. 10.



10  $\mu$

ZN-4536

Fig. 11

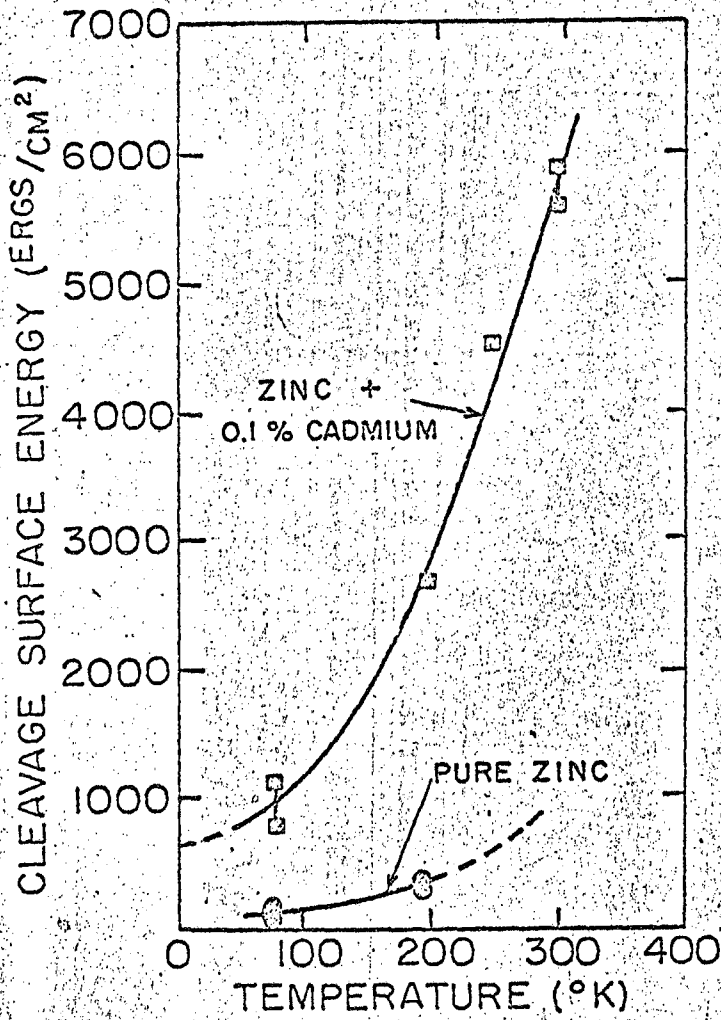


Fig. 12.

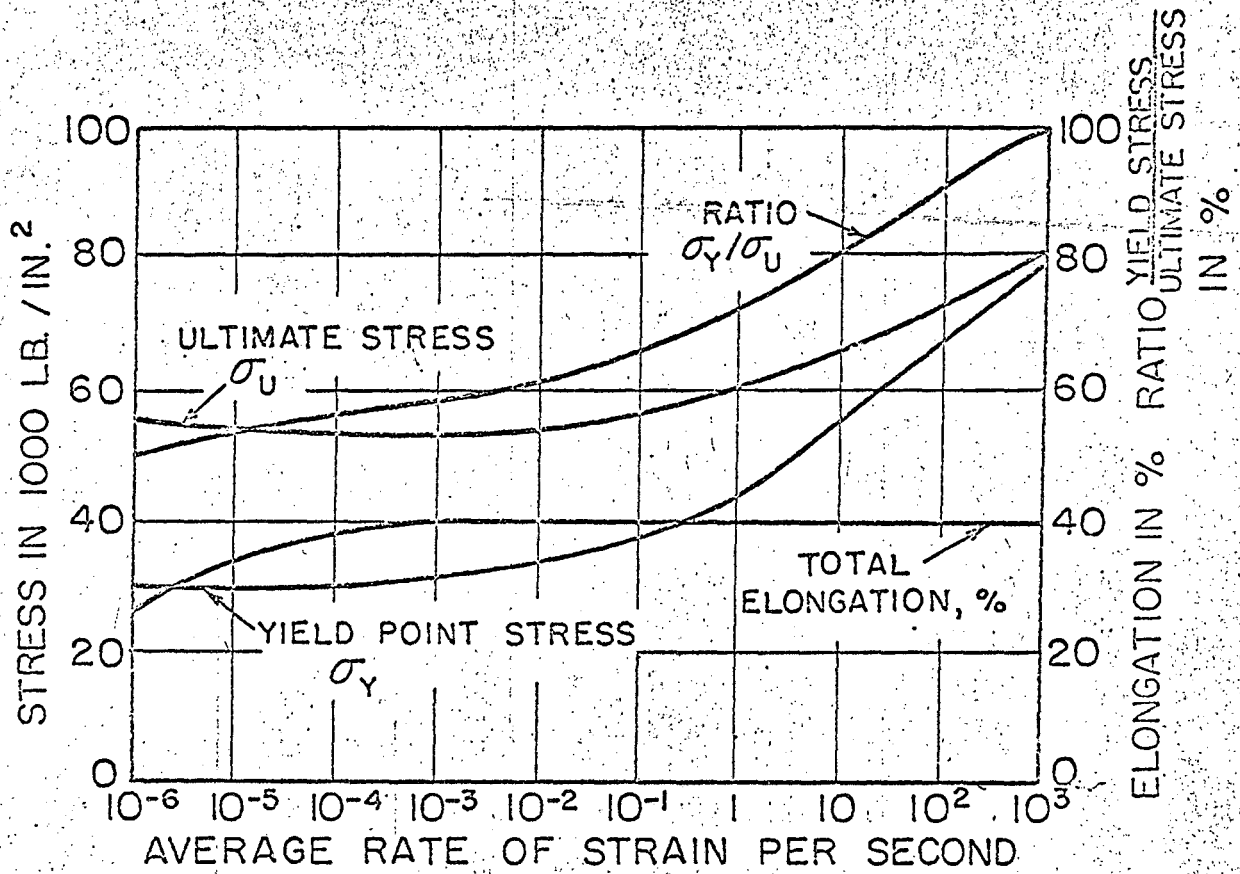


Fig. 13.



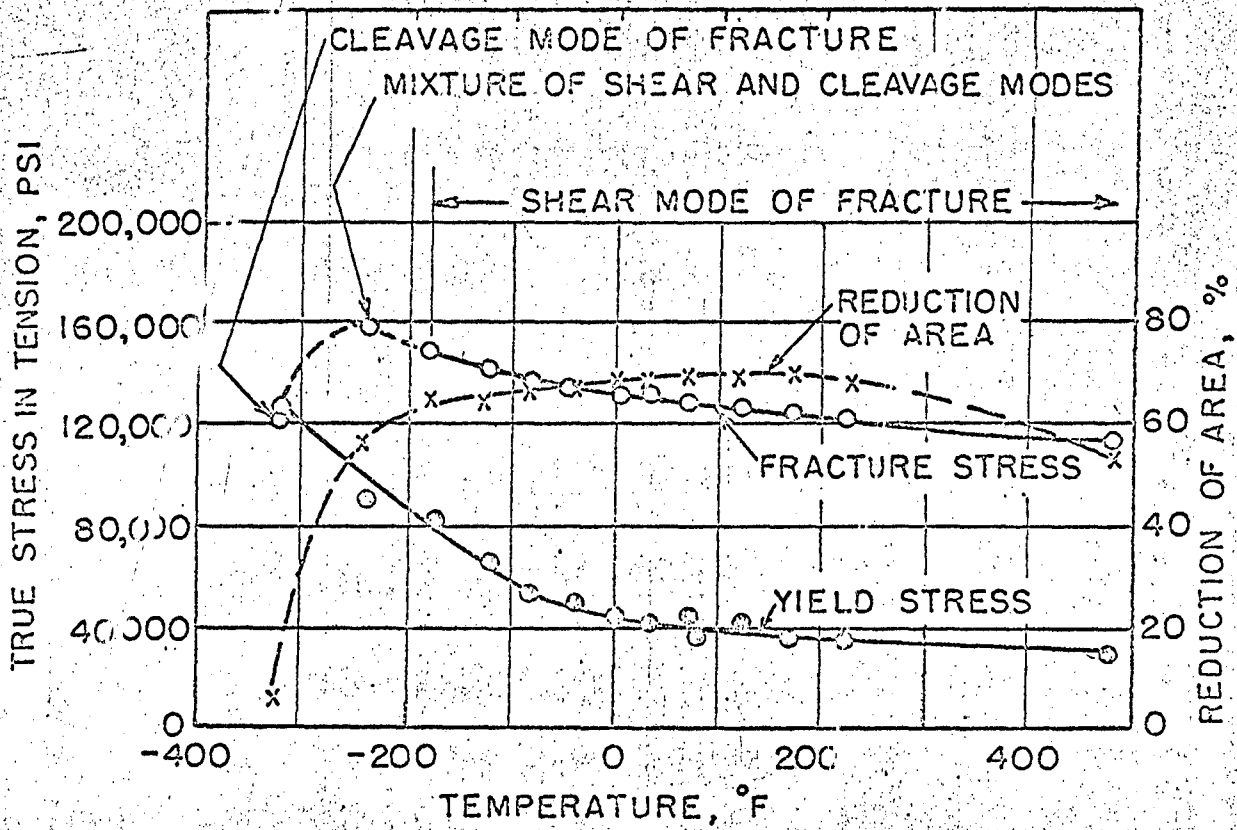


Fig. 14.

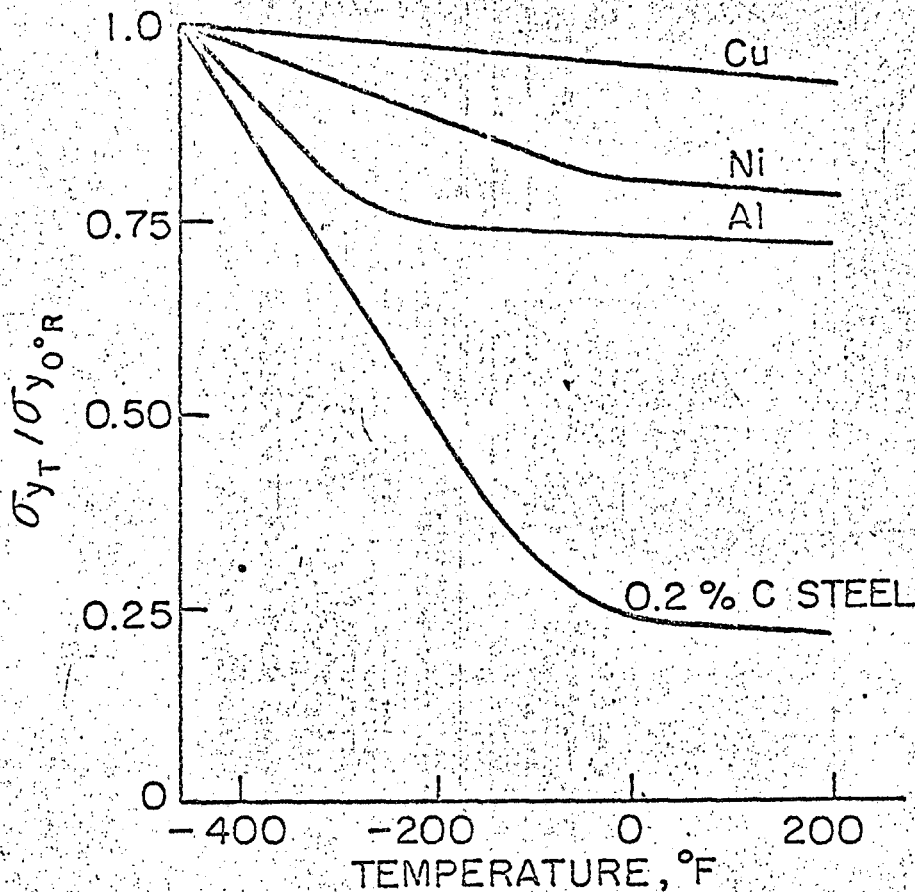
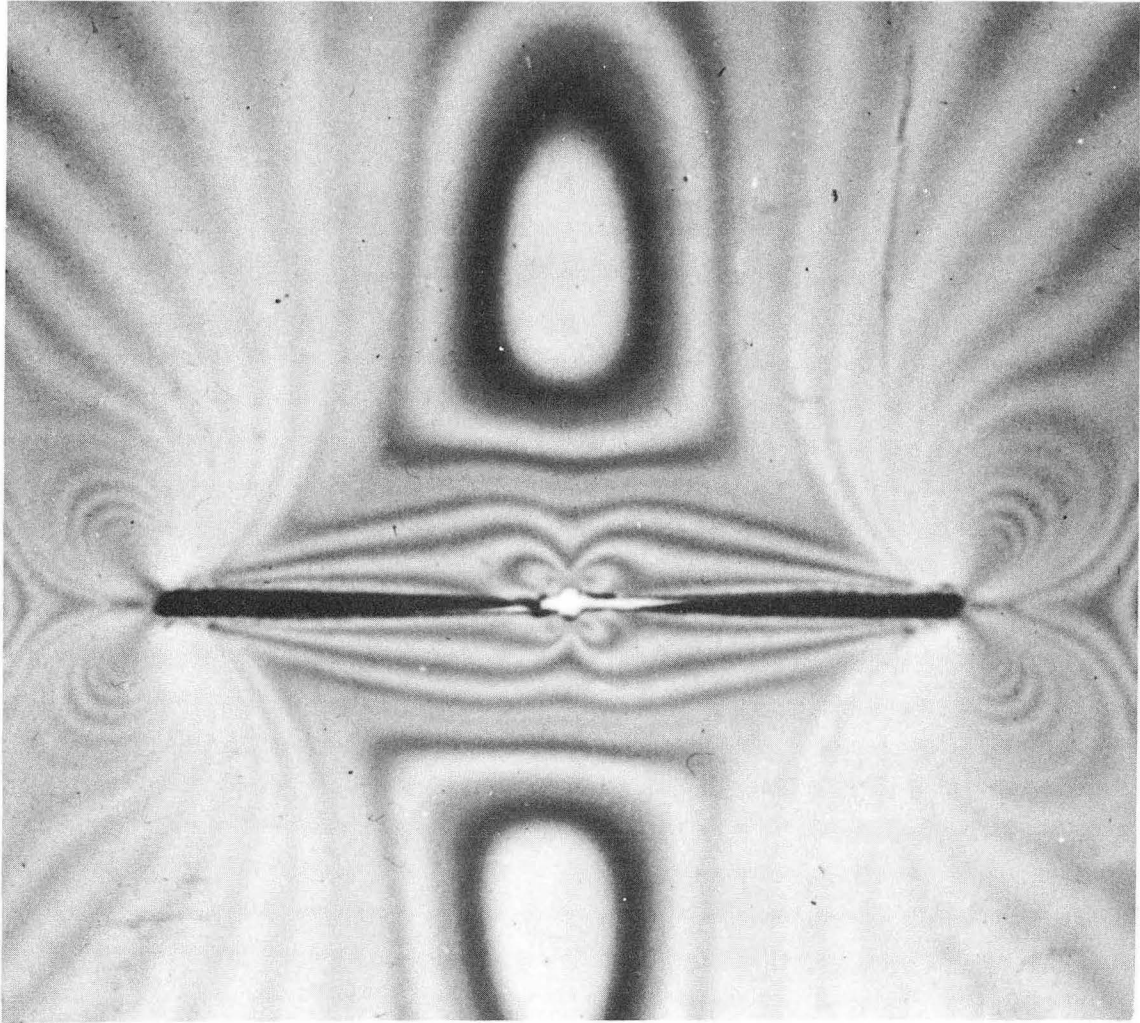


Fig. 15.





ZN-4532

Fig. 16

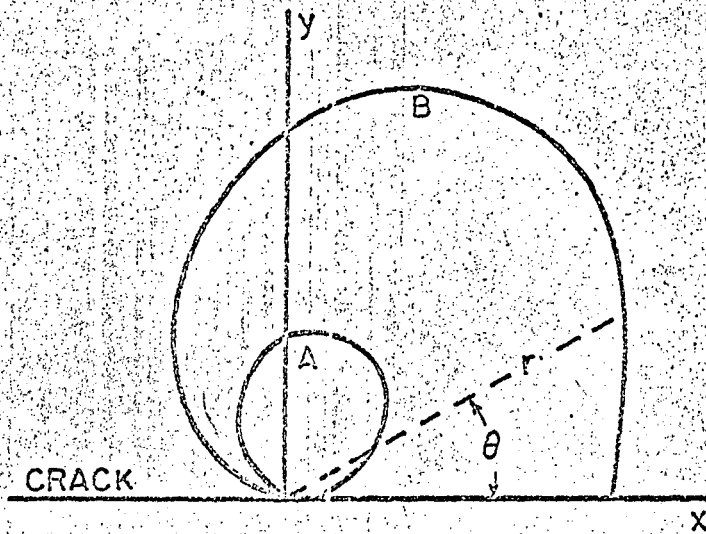


Fig. 17.

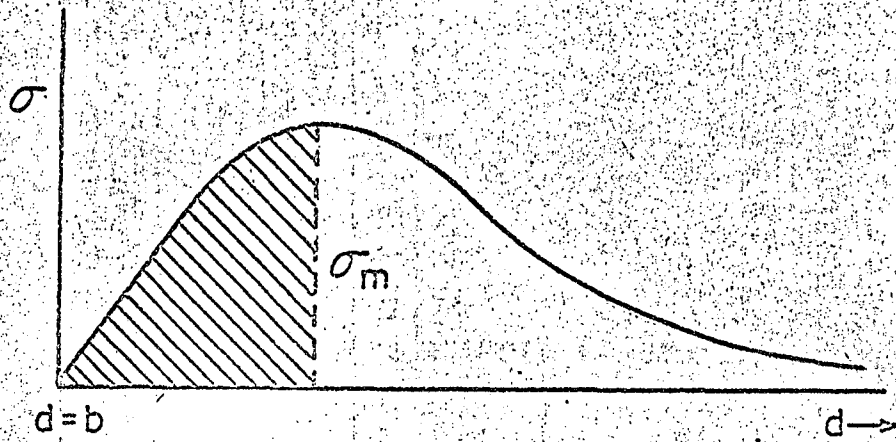


Fig. 18.

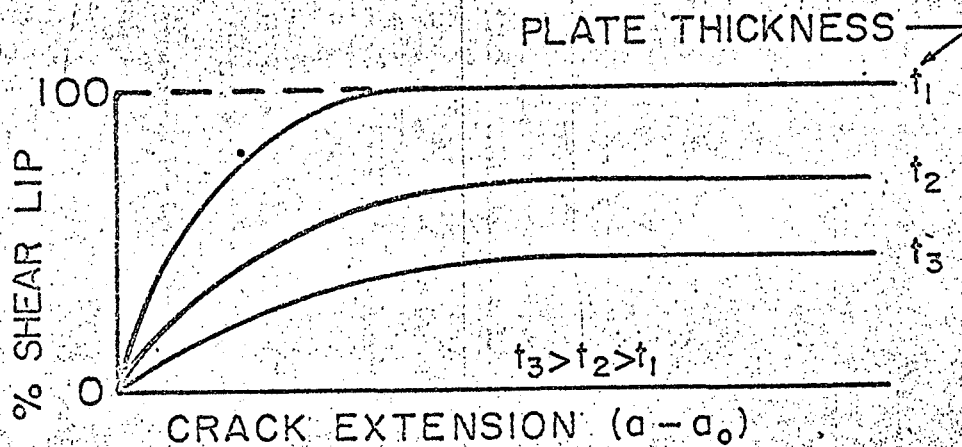
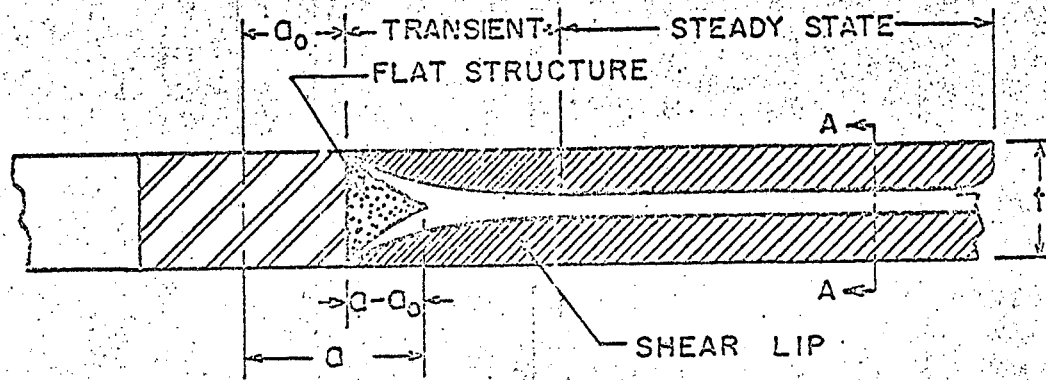


Fig. 19.

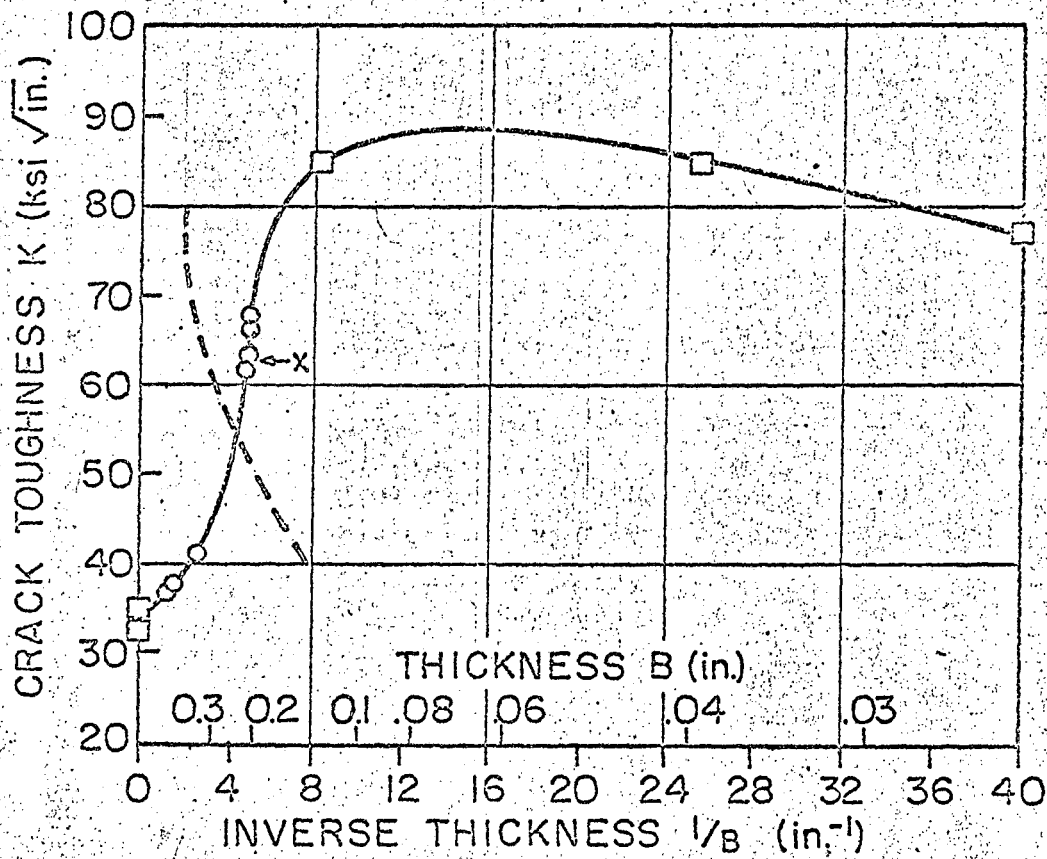


Fig. 20.



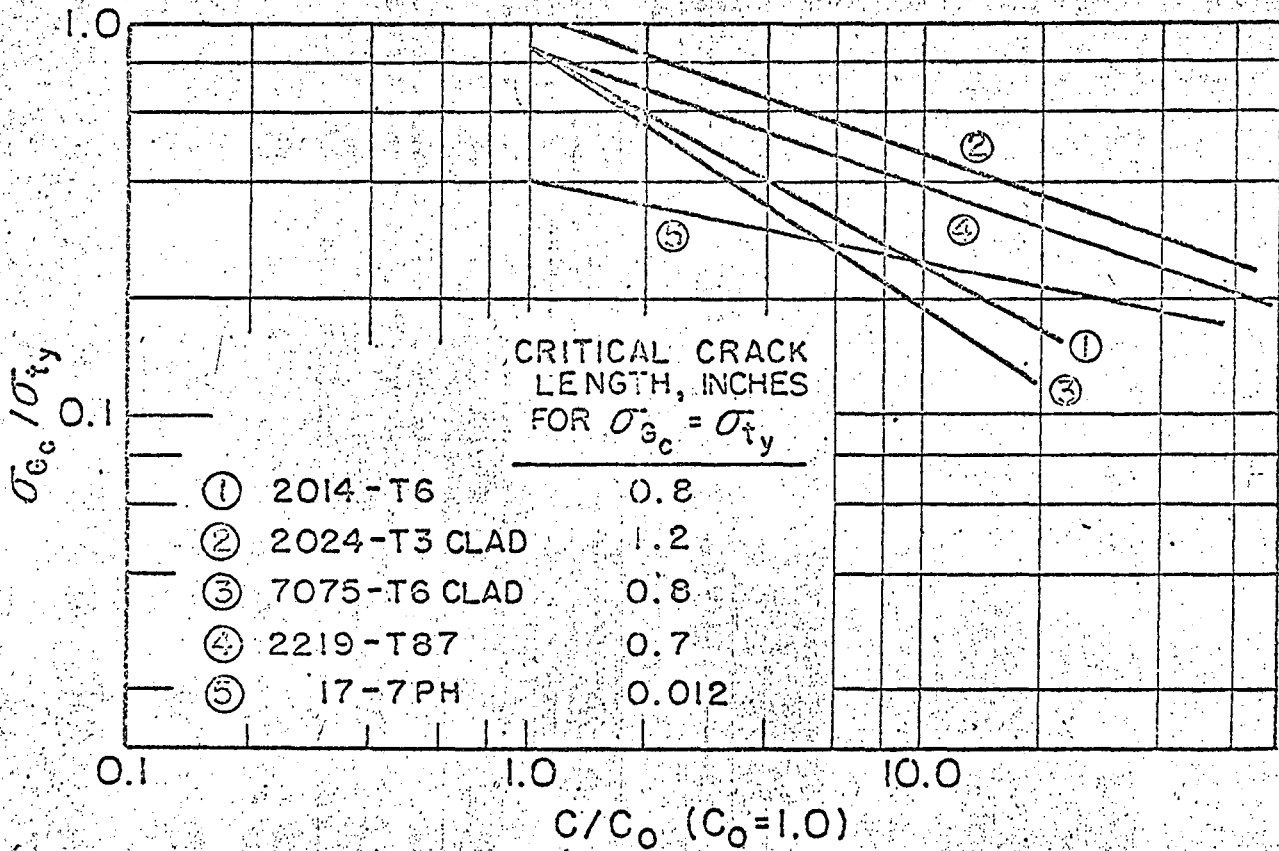
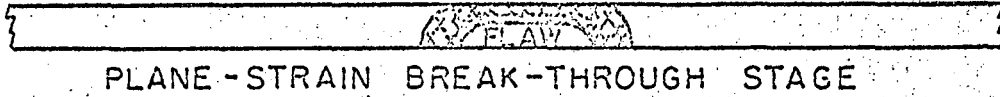


Fig. 21.

Fig. 21

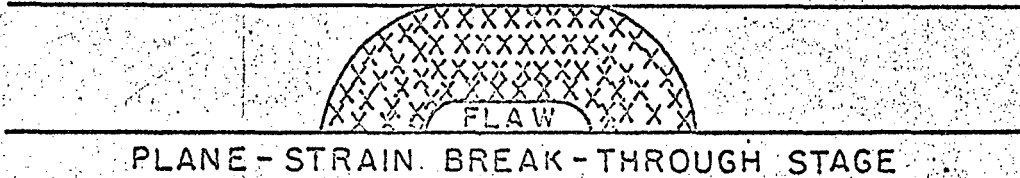


PLANE - STRAIN BREAK - THROUGH STAGE

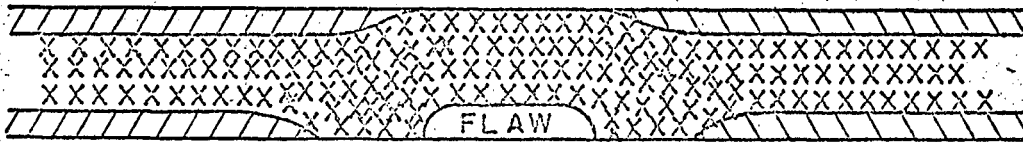


PLANE - STRESS GROWTH STAGE

THIN PLATE



PLANE - STRAIN BREAK - THROUGH STAGE



COMPLEX GROWTH STAGE

THICK PLATE

Fig. 22.

This report was prepared as an account of Government sponsored work. Neither the United States, nor the Commission, nor any person acting on behalf of the Commission:

- A. Makes any warranty or representation, expressed or implied, with respect to the accuracy, completeness, or usefulness of the information contained in this report, or that the use of any information, apparatus, method, or process disclosed in this report may not infringe privately owned rights; or
- B. Assumes any liabilities with respect to the use of, or for damages resulting from the use of any information, apparatus, method, or process disclosed in this report.

As used in the above, "person acting on behalf of the Commission" includes any employee or contractor of the Commission, or employee of such contractor, to the extent that such employee or contractor of the Commission, or employee of such contractor prepares, disseminates, or provides access to, any information pursuant to his employment or contract with the Commission, or his employment with such contractor.



